NASA Technical Memorandum 104274

Strain Gage Measurement Errors in the Transient Heating of Structural Components

W. Lance Richards

December 1993

National Aeronautics and
Space Administration

NASA Technical Memorandum 104274

Strain Gage Measurement Errors in the Transient Heating of Structural Components

W. Lance Richards
NASA Dryden Flight Research Facility
Edwards, California

1993

National Aeronautics and
Space Administration

Dryden Flight Research Facility
Edwards, California 93523-0273

STRAIN GAGE MEASUREMENT ERRORS IN THE TRANSIENT HEATING OF STRUCTURAL COMPONENTS

ABSTRACT

Significant strain-gage errors may exist in measurements acquired in transient thermal environments if conventional correction methods are applied. Conventional correction theory was modified and a new experimental method was developed to correct indicated strain data for errors created in radiant heating environments ranging from 0.6 °C/sec (1 °F/sec) to over 56 °C/sec (100 °F/sec). In some cases the new and conventional methods differed by as much as 30 percent. Experimental and analytical results were compared to demonstrate the new technique. For heating conditions greater than 6 °C/sec (10 °F/sec), the indicated strain data corrected with the developed technique compared much better to analysis than the same data corrected with the conventional technique.

NOMENCLATURE

a	coefficient
CTE	coefficient of thermal expansion
DACS	data acquisition and control system
GF	gage factor
T	temperature, °C
z	coordinate through the thickness of the coupon
α	coefficient of thermal expansion, ppm/°C
γ	thermal coefficient of resistance, ppm/°C
ΔT	temperature change from initial temperature, °C
ε_{app}	apparent strain, µstrain
ε_{ind}	indicated strain, µstrain
ε_{th}	transient heating error, µstrain
$\varepsilon_{\Sigma T}$	total strain error due to temperature, µstrain
ε_{σ}	stress-induced strain, µstrain

Subscripts

g	gage
$g - s$	difference between gage and substrate
s	substrate
x,y	rectangular coordinates in the plane of the coupon

INTRODUCTION

The techniques used to correct strain-gage errors encountered in slowly varying heating environments are well established. However, many experimental programs, like those that simulate aerodynamic heating, require test articles instrumented with electrical resistance strain gages to be exposed to extremely high heating rates. This is especially true for tests in support of hypersonic or transatmospheric vehicles. Figure 1 shows such a vehicle test component instrumented with a bonded electrical resistance strain gage. As heating rates increase, the temperature gradient between the strain gage filament and the substrate increases according to Fourier’s law. This temperature difference, shown in Figure 1 as ΔT, becomes increasingly significant because backing materials used to insulate gages electrically from the substrate are usually good thermal insulators as well. Therefore, the lower the thermal conductivity of the insulating material, the greater the temperature difference between the gage filament and the substrate becomes (for the same imposed heat flux). Conventional strain correction procedures currently neglect this temperature gradient by assuming that the strain gage sensing filament and the substrate temperatures are equal. Consequently, significant errors may be neglected in strain indications acquired in transient environments.

Limited information is available in the literature concerning the correction of electrical-resistance strain-gage measurement errors produced specifically by transient heating. Part of a study Wilson conducted for the X-15 program [1] evaluated weldable strain-gage performance to 482 °C (900 °F) with heating rates of 0.9, 2.8, and 6 °C/sec (1.7, 5, and 10 °F/sec). Adams [2] evaluated the weldable strain-gage response in a heating simulation of a sodium spill in a reactor pressure vessel. Temperatures greater than 538 °C (1000 °F) and heating rates of approximately 56 °C/sec (100 °F/sec) were obtained. These studies only addressed weldable strain-gage behavior and employed methods not easily adapted to other test programs. No studies were found in the literature that either defined the strain errors produced in transient conditions or provided general techniques to correct errors if they were significant. The objectives of this investigation are, therefore, to understand foil strain-gage measurements acquired in a variety of rapid heating environments and to develop a correction method generally applicable to many current test programs.

BACKGROUND

This section reviews the conventional strain correction theory by defining the most significant measurement error present in elevated temperature environments. The experimental procedures used to account for this error are also reviewed.

Conventional Correction Theory

The strain-gage indication in elevated temperature environments consists of essentially two components as shown in the following equation

$$\varepsilon_{ind}(T_i) = \varepsilon_{\sigma}(T_i) + \varepsilon_{app}(T_i) \tag{1}$$

Each term in this equation is expressed as a function of the temperature range at any given point, T_i. This first component, ε_σ is the stress-induced strain and corresponds to the true stress state-of-the-test article. These strains may result from nonuniform thermal gradients, externally applied mechanical loads, or a combination of both. Ideally, the strain-gage sensor should sense only stress-induced strains. However, in extreme heating conditions, the gage also responds to apparent strain; the second component in equation (1). This error is defined by the following equation [3]

$$\varepsilon_{app} = \left[(\alpha_s - \alpha_g) + \frac{\gamma}{GF}\right]\Delta T_s \tag{2}$$

Other less significant errors such as gage factor variation with temperature, Wheatstone bridge nonlinearity, transverse sensitivity, lead wire desensitization, etc., may also exist in equation (1). These errors, however, are assumed to have been already accounted for using conventional methods. The errors and the correction methods are beyond the scope of this study.

Conventional Correction Procedure

The common technique for characterizing apparent strain is to conduct isothermal temperature tests on coupons made from the same material batch as the test article. Ideally these coupons have experienced the same processes and heat treatments as the test article material so that they adequately represent the test article material behavior. The coupon material is instrumented with the same strain gages to be installed on the test article. A thermocouple is spot-welded to the coupon near the strain-gage location which, for the conventional procedure, is assumed to measure the coupon and gage temperatures. The unrestrained coupon is then heated slowly to ensure that the coupon is free of thermal stress. The strain-gage output over the expected temperature range is the apparent strain output. The stress-induced strain produced in the test article during an actual test is then determined by subtracting the isothermal apparent strain error from the indicated strain measurement (ε_{ind}). In equation form, this means solving equation (1) for ε_σ at each point in the temperature profile.

APPROACH

The conventional theory and procedure used to correct the strain-gage indication are based on the assumption that the temperature environment varies so slowly that the gage and the substrate temperatures remain the same. This section first adapts the conventional correction theory to represent the more general heating case when the gage and the substrate temperatures are different. In addition to the usual strain errors previously discussed, a new error is identified which reflects the strain error produced in transient heating conditions. After modifying the conventional strain correction theory, a new procedure is presented.

New Correction Theory

If the heating rates are sufficiently severe, the strain-gage indication shown in equation (1) will contain another error, referred to in this report as the transient heating error (ε_{th}). Adding this term to equation (1) yields

$$\varepsilon_{ind}(T_i) = \varepsilon_{\sigma}(T_i) + \varepsilon_{app}(T_i) + \varepsilon_{th}(T_i) \tag{3}$$

(Since these terms are functions of temperature, the temperature dependence expression T_i will not be used in subsequent equations). The last term in equation (3) can be derived by first separating the terms caused by substrate effects from those caused by gage effects in the apparent strain relationship expressed in equation (2).

$$\varepsilon_{app} = \underbrace{\alpha_s \Delta T_s}_{\text{substrate}} + \underbrace{\left(\frac{\gamma}{GF} - \alpha_g\right)\Delta T_s}_{\text{gage}} \tag{4}$$

A temperature difference (ΔT_{g-s}) is then added to the gage component of equation (4) and the right-hand side is redefined to be the total strain error caused by any elevated temperature environment ($\varepsilon_{\Sigma T}$).

After rearranging terms, this equation becomes

$$\varepsilon_{\Sigma T} = \left[(\alpha_s - \alpha_g) + \frac{\gamma}{GF}\right] \Delta T_s + \left(\frac{\gamma}{GF} - \alpha_g\right)\Delta T_{g-s} \tag{5}$$

where the second term in this equation is the transient heating error

$$\varepsilon_{th} = \left(\frac{\gamma}{GF} - \alpha_g\right)\Delta T_{g-s} \tag{6}$$

and the first term in equation (5) represents the apparent strain defined in equation (2). Substituting equations (2) and (6) into equation (5) yields

$$\varepsilon_{\Sigma T} = \varepsilon_{app} + \varepsilon_{th} \tag{7}$$

If all the coefficients in equation (5) were known as functions of temperature, then these errors could be calculated directly. Since the gage material properties are not accurately known, the total strain error due to temperature ($\varepsilon_{\Sigma T}$) and the transient heating error (ε_{th}) must be determined through empirical methods. Recognizing that $\Delta T_{g-s} = \Delta T_g - \Delta T_s$, solving for ΔT_s and substituting into equation (5) produces the following expression

$$\varepsilon_{\Sigma T} = \varepsilon_{app}\left(\frac{\Delta T_g}{\Delta T_s}\right) - \alpha_s \Delta T_{g-s} \tag{8}$$

Equation (8) is the empirical relationship required to correct strain measurement errors produced in the most general heating environment; those errors produced in isothermal and transient environments. As the temperature environment approaches isothermal conditions, the ΔT_{g-s} term approaches zero and the bracketed term approaches unity. Therefore the total strain error due to temperature approaces the conventional definition of apparent strain as the transient heating environment approaches isothermal conditions.

New Correction Procedure

Figure 2 presents the new and conventional correction procedures. The conventional procedure is on the left, the new procedure on the right, and steps that both procedures have in common are in the center. The first step in both correction procedures is to characterize the apparent strain error using the conventional methods described previously. Both procedures then require the apparent strain coupon to be instrumented with the same type of gages and thermocouples to be installed on the test component. The new procedure, however, requires an indication of the strain-gage filament temperature during the transient heating tests. In this approach, the gage temperature is represented by installing a foil thermocouple near the strain gage using the same attachment materials and techniques as the foil strain gages. The foil thermocouple is assumed to represent the gage temperature (ΔT_g) because of their similar materials and construction. Figure 3 shows that the foil strain gage and foil thermocouple cross-sections are nearly identical, with the largest difference being the 0.0008-cm (0.0003-in.) difference between the foil strain-gage filament and thermocouple foil.

The next step in both procedures is to conduct the transient heating tests on the test component. To determine the strain state of the test component, the conventional procedure simply subtracts the apparent strain result from the transient test data. The new procedure, however, first determines ΔT_{g-s} at each time in the transient heating test and then determines the total strain error due to temperature and the transient heating error as shown in Figure 2. The transient heating error and apparent strain are subtracted from the indicated strain measurement to determine the stress-induced strain in the test component.

TEST DESCRIPTION

A series of tests were conducted to demonstrate the new correction theory and experimental procedure. This section describes the test coupon and instrumentation and the test matrix used in the experiment. The data acquisition and control system used in the tests is described in Reference 4.

Test Coupons–Instrumentation

A titanium coupon (5Al-2.5Sn alloy) measuring $7.62 \times 12.7 \times 0.635$ cm ($3 \times 5 \times 0.25$ in.) was first used to characterize apparent strain using conventional methods. The same coupon also served as the “test component” in the transient heating tests.

For the apparent strain tests, the coupon was instrumented with type-K thermocouples and Micro-Measurements (Raleigh, North Carolina) foil strain gages (WK-05-125BZ-10C) as shown in Figure 4. The rectangular strain-gage rosette, shown in the middle of the coupon, was installed to provide an adequate statistical representation of the apparent strain error. The spot-welded thermocouple at the intersection of the three strain axes is normally assumed to measure the strain-gage temperatures for isothermal apparent strain tests. The gage installation, together with its corresponding thermocouple, is typical of isothermal apparent strain-gage evaluations.

In addition to the instrumentation previously described, the transient heating tests also required that type-K foil thermocouples (RdF Corp., Hudson, New Hampshire) be bonded to the substrate (see Fig. 4) using the same attachment materials and techniques as the foil strain gages discussed earlier. The difference between the foil and spot-welded thermocouple measurements defines the ΔT_{g-s} term used in the total strain error due to temperature (eq. (5)). The instrumentation shown on the top surface in Figure 4 has corresponding sensors located on the bottom surface. A total of 30 spot-welded thermocouples, 2 foil thermocouples and 6 foil strain gages were used in the tests. Before the transient heating tests, the instrumented coupon shown in Figure 4 was painted with a high-emittance paint (not shown). This helped to ensure that a uniform heat flux was applied to the coupon surface and also helped to improve the radiative heating efficiency.

Test Matrix

Table 1 shows a matrix of the various heating rates applied to the coupon, the number of tests per heating rate, the maximum temperature obtained, and the data acquisition sampling rate in the test program.

Table 1. Test matrix: number of tets and maximum temperature as functions of heating rate.

	Heating rate, °C/sec (°F/sec)							
	0.2 (0.3)	0.6 (1)	2.8 (5)	6 (10)	11 (20)	22 (40)	44 (80)	56 (100)
Number of tests	4	4	5	6	5	5	4	2
Max. temp., °C (F)	316 (600)	316 (600)	316 (600)	316 (600)	316 (600)	260 (500)	232 (450)	204 (400)
Sampling rate, sps	1	12	12	12	12	12	144	144

The strain data for the 0.2 °C/sec (0.3 °F/sec) tests were corrected using conventional methods and were used as the baseline apparent strain correction. The coupon was heated by convection for the 0.2 °C (0.3 °F) tests and was heated by radiation for all other tests. The data sampling rate, initially at 1 sample per second (sps) for the 0.2 °C/sec (0.3 °F/sec) was increased to 12 sps, and eventually to 144 sps to acquire a sufficient number of data samples at the higher heating rates.

TEST RESULTS

Transient heating error results for a single, representative test at each heating rate between 6 °C/sec (10 °F/sec) and 56 °C/sec (100 °F/sec) are presented. Transient errors for tests with heating rates less than or equal to 2.8 °C/sec (5 °F/sec) were found to be negligible and are therefore not presented.

Transient Heating Error Results

The transient heating errors shown in Figure 5 and Table 2, illustrate the significance of the errors that are produced using the conventional correction methods; especially for the 44 °C/sec (80 °F/sec) and 56 °C/sec (100 °F/sec) tests as shown in Figure 5(b). For these tests, the magnitude of the transient heating error is of the same order as the apparent strain response itself which is shown in Table 3. Since apparent strain is an error that usually drives the accuracy of strain measurements in elevated temperature conditions, neglecting an error of comparable value may lead to grossly inaccurate strain measurements.

Table 2. Transient heating error (ε_{th}) for various heating rates and temperatures.

			Transient heating errors, μstrain, at various temperatures					
			38 °C (100 °F)	93 °C (200 °F)	149 °C (300 °F)	204 °C (400 ° F)	260 °C (500 °F)	316 °C (600 °F)
Heating rate, °C/sec (°F/sec)	6	(10)	–8	–8	0	–8	–26	–40
	11	(20)	–16	–28	–18	–26	–40	–56
	22	(40)	–30	–45	–25	–40	–65	– – –
	44	(80)	–30	–95	–50	–100	– – –	– – –
	56	(100)	–15	–165	–170	– – –	– – –	– – –

Table 3. Apparent strain (ε_{app}) at various temperatures.

			Apparent atrain, μstrain, at various temperatures					
			38 °C (100 °F)	93 °C (200 °F)	149 °C (300 °F)	204 °C (400 ° F)	260 °C (500 °F)	316 °C (600 °F)
Heating rate, °C/sec (°F/sec)	0.2	(0.3)	50	130	125	65	–45	–170

It should be noted that Table 2 does not present error values for some of the elevated temperatures at the higher heating rates. This is because the measured strains at the higher temperatures increased significantly as the heating rate was increased. For example, at 260 °C (500 °F), some of the indicated strain data obtained at higher heating rates were in the neighborhood of –10,000 μstrain and were increasing rapidly. The upper temperature limits proposed for the higher heating rate tests were therefore lowered to avoid exceeding the 15,000-μstrain limit of the gage. For these gages, the maximum usage temperatures were determined to be approximately 260, 204, and 177 °C (500, 400, and 350 °F) at heating rates of 22, 44, and 56 °C/sec (40, 80, and 100 °F/sec) respectively. Although the upper temperature limit of the strain gage is given by the manufacturer as 288 °C (550 °F), this limit was not appropriate for heating rates at or above 22 °C/sec (40 °F/sec).

Although the correction method presented in this study is intended to be general, the transient heating error results shown in Figure 5 and Table 2 are specific to this study. These data are presented for qualitative comparisons only. The transient heating error is highly dependent on the temperature change of the gage, and since the time constant of the gage is so small, even a slight variation in the temperature profile from one test to another will greatly affect the characteristics of the error. This is clearly illustrated by the fluctuating results in the 22 °C/sec (40 °F/sec) and 44 °C/sec (80 °F/sec) cases shown in Figure 5. For these two cases, the temperature control was especially sporadic, causing the foil thermocouple measurements to lead the spot-welded thermocouple measurements during heating surges and lag during cooling. This wildly fluctuating temperature difference is used to calculate the transient heating error as shown in Figure 5.

ANALYTICAL DEMONSTRATION OF NEW APPROACH

To demonstrate the new approach adequately, the stress-induced strains produced in the coupon for the various transient heating rates were determined through an analysis and then compared with the results from both experimental methods. The analysis was required to first determine the temperature distribution through the coupon thickness, since these measurements were experimentally impractical. Temperature distributions of the form shown in equation (9) were determined using the finite difference model shown in Figure 6.

$$T(z) = a_0 + a_1 z + a_2 z^2 + a_3 z^3 \tag{9}$$

The temperatures were then substituted into the governing thermal stress equation [5]. Using generalized Hooke's law, the following relationship for principal strains was determined

$$\varepsilon_x = \varepsilon_y = \alpha_s \left[a_2 \left(\frac{t^2}{12} - z \right) + a_3 \left(\frac{3}{20} t^3 z \right) \right] \tag{10}$$

Strains calculated from equation (10) were compared directly with measured strains corrected with both experimental methods.

Comparison of Experimental and Analytical Results

Figure 7 compares the experimental and analytical results for typical 6, 22, 44, and 56 °C/sec (10, 40, 80, and 100 °F/sec) heating rate tests. Good correlation between the test and analytical results was obtained for tests greater than 6 °C/sec (10 °F/sec). The 6 °C/sec (10 °F/sec) case compared moderately well with analysis, given the relatively small magnitudes of the apparent strain output for this case. The results from this case show that there is no advantage in using the new correction procedure at or below this heating rate. It is suspected for the lower heating rates that the foil and substrate temperature measurements are not accurate enough to warrant further correction. Figures 7(b) through 7(d) show that the new method produces much better agreement with analysis than the conventional methods. Although the new method agreed only moderately well with the 22 °C/sec (40 °F/sec) analysis, the new method was still 27 percent better than if conventional methods were used. In the 44 °C/sec (80 °F/sec) and 56 °C/sec (100 °F/sec) heating rate tests, the conventional method yielded strain measurements that were off by approximately 30 percent. Excellent agreement between the new method and analysis is shown in these cases.

CONCLUSIONS

A strain measurement error which is produced in transient heating environments was mathematically and experimentally defined. The significance of this error was demonstrated for a reliable high-temperature foil strain-gage installation subjected to a variety of radiantly heated, transient temperature profiles. For heating rates between 6 °C/sec (10 °F/sec) and 56 °C/sec (100 °F/sec), the error due to transient heating was as significant as apparent strain; the most significant strain error occurring in extreme temperature environments. However, for heating rates less than 6 °C/sec (10 °F/sec), the error was negligible. The transient heating error was found to be extremely sensitive to the specific heating profile applied in a given test.

Although the transient heating error results were specific to this study, the correction technique used to determine the errors is generally applicable to other experimental programs which have different instrumentation and heating requirements. The new strain correction technique was developed and successfully demonstrated with analysis. For all heating rates greater than 6 °C/sec (10 °F/sec), the new technique produced strain measurements which compared much better to analysis than measurements obtained with the conventional technique.

REFERENCES

1. Wilson, Earl J., "Installation and Testing of Strain Gages for High-Temperature Aircraft Applications," Society for Experimental Stress Analysis, Fall Meeting, Oct. 18–22, 1970.
2. Adams, P.H., "Transient Temperature Response of Strain Gages," SAND-80-2689-REV-1, Centrifuge, Climatic and Radiant Heat Division 7531, Sandia National Laboratories, Albuquerque, NM,1983.
3. Dally, James W. and Riley, William F., "Experimental Stress Analysis," Second Edition, McGraw-Hill Book Co., NY, NY, 1978, pp. 153–178.
4. Zamanzadeh, Behzad, Trover, William F., and Anderson, Karl F., "DACS II - A Distributed Thermal/Mechanical Loads Data Acquisition and Control System," International Telemetring Conference, San Diego, CA, July 1987.
5. Boley, Bruno A. and Weiner, Jerome H., "Theory of Thermal Stresses," Reprint Edition (1985), Robert E. Krieger Publishing Co. Inc., Malabar, FL, John Wiley & Sons, Inc., New York.

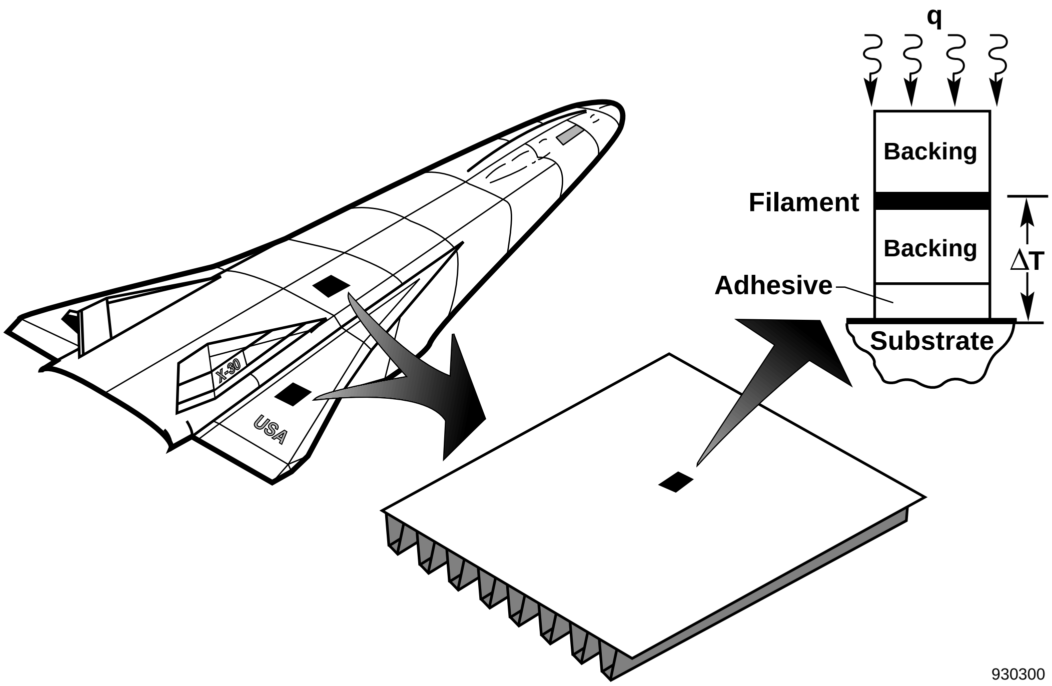

Figure 1. Strain gage installation on a hypersonic vehicle test component.

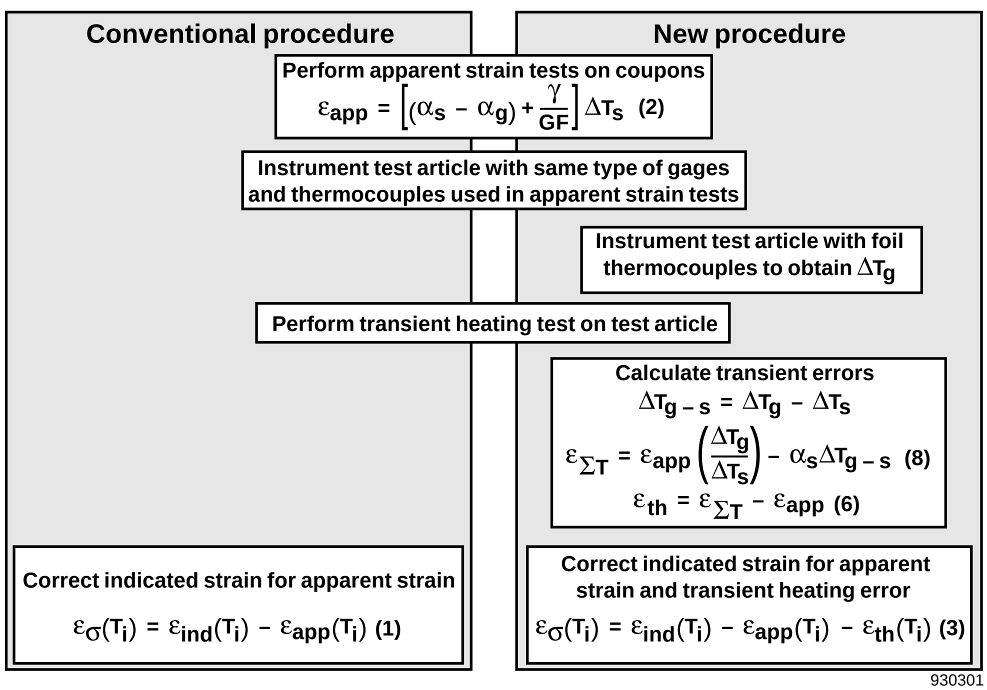

Figure 2. New and conventional correction procedures.

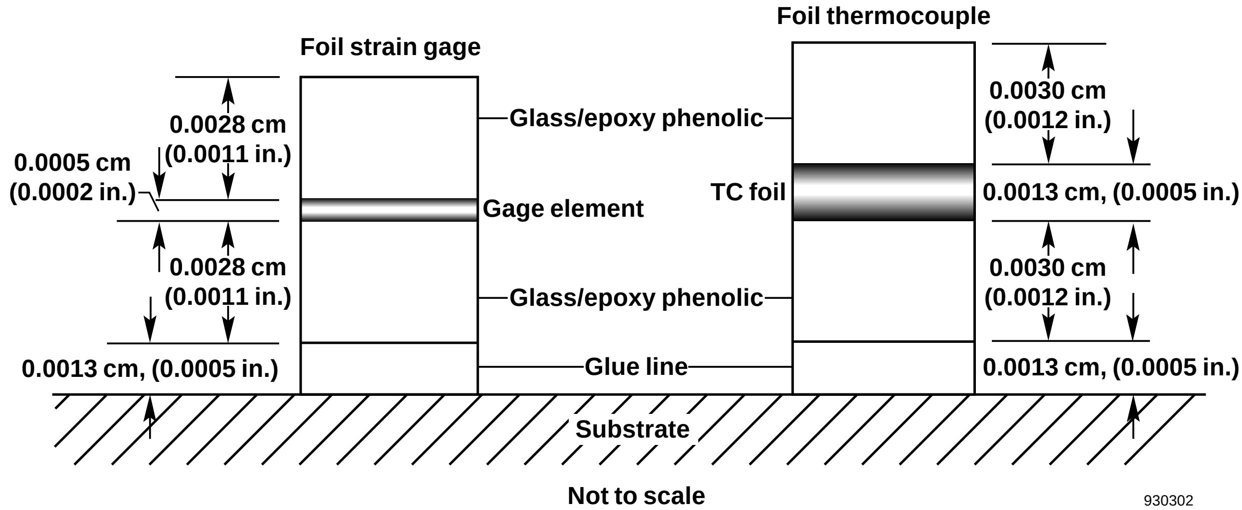

Figure 3. Comparision of foil strain gage and foil thermocouple cross-sections.

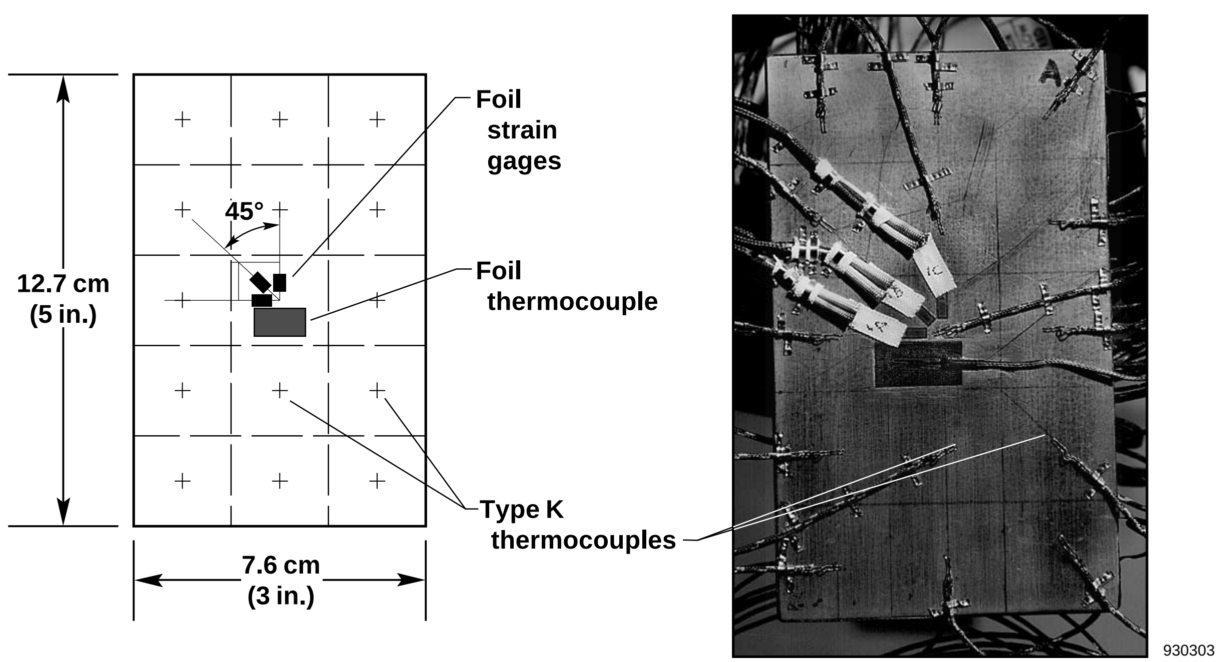

Figure 4. Test coupon and instrumentation.

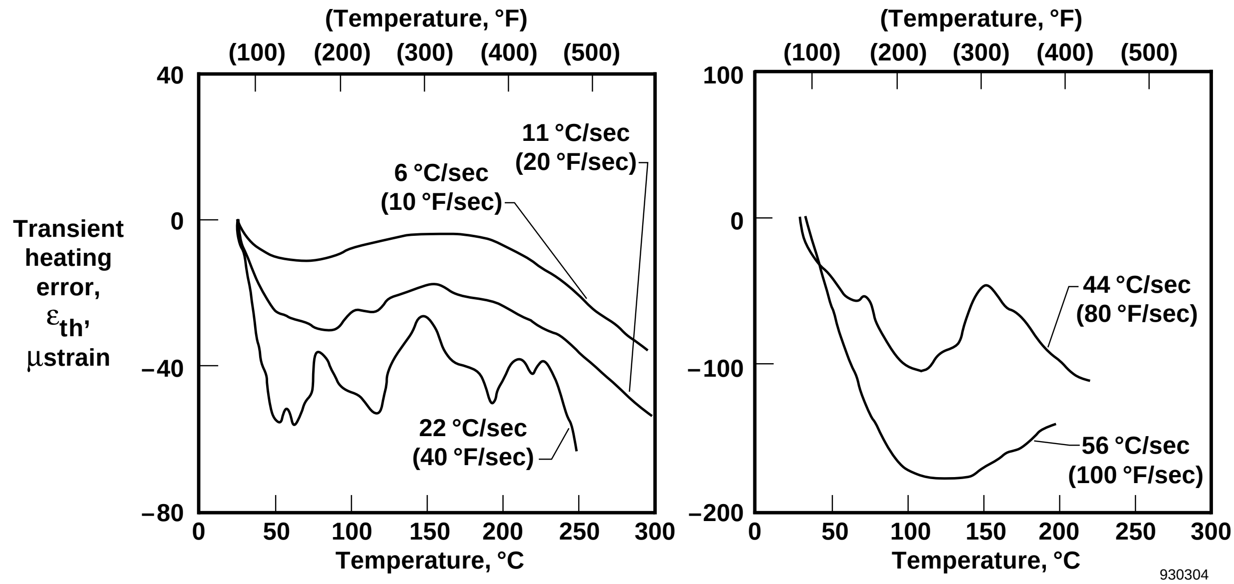

Figure 5. Transient heating error results.

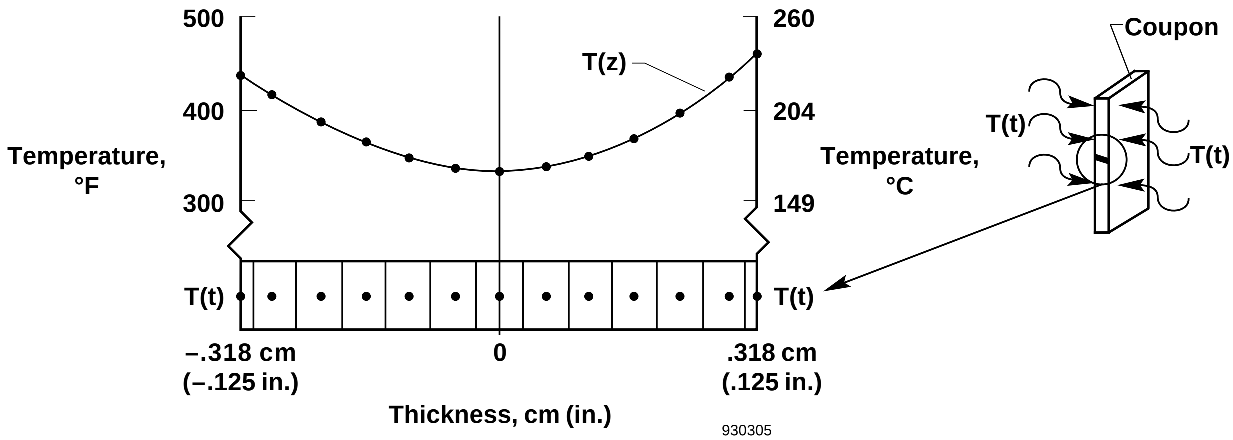

Figure 6. Finite-difference model.

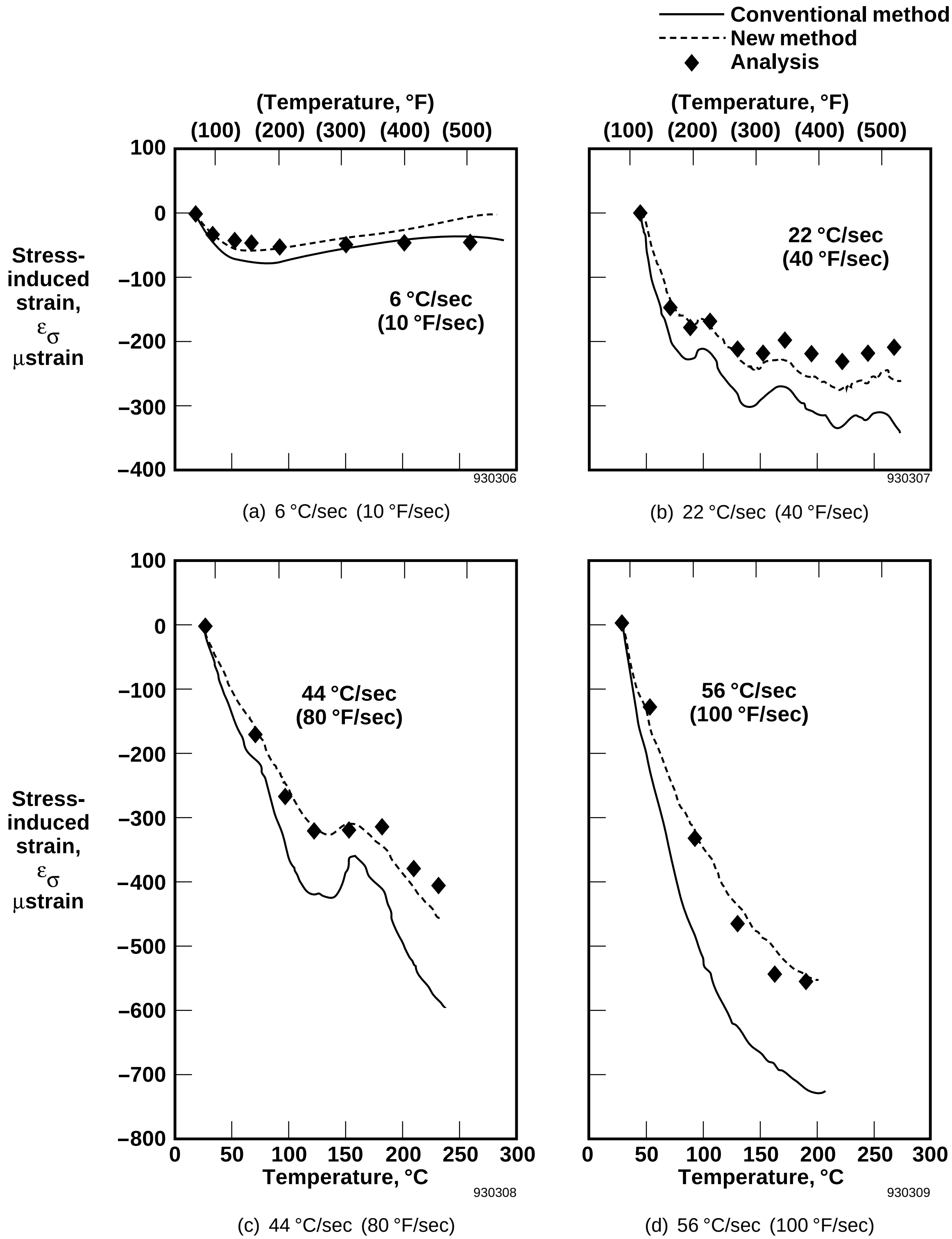

Figure 7. Stress-induced strain comparisons.

REPORT DOCUMENTATION PAGE

Form Approved
OMB No. 0704-0188

1. AGENCY USE ONLY (Leave blank)	2. REPORT DATE	3. REPORT TYPE AND DATES COVERED
	December 1993	Technical Memorandum

4. TITLE AND SUBTITLE

Strain Gauge Measurement Errors in the Transient Heating of Structural Components

5. FUNDING NUMBERS

WU 505-70-63

6. AUTHOR(S)

W. Lance Richards

7. PERFORMING ORGANIZATION NAME(S) AND ADDRESS(ES)

NASA Dryden Flight Research Facility
P.O. Box 273
Edwards, California 93523-0273

8. PERFORMING ORGANIZATION REPORT NUMBER

H-1960

9. SPONSORING/MONITORING AGENCY NAME(S) AND ADDRESS(ES)

National Aeronautics and Space Administration
Washington, DC 20546-0001

10. SPONSORING/MONITORING AGENCY REPORT NUMBER

NASA TM-104274

11. SUPPLEMENTARY NOTES

Prepared as a conference paper for the SEM Fall Conference and Exhibit - Structural Testing at High Temperature II, Ojai, CA, Nov. 8–10, 1993.

12a. DISTRIBUTION/AVAILABILITY STATEMENT

Unclassified—Unlimited
Subject Category 39

12b. DISTRIBUTION CODE

13. ABSTRACT (Maximum 200 words)

Significant strain-gage errors may exist in measurements acquired in transient thermal environments if conventional correction methods are applied. Conventional correction theory was modified and a new experimental method was developed to correct indicated strain data for errors created in radiant heating environments ranging from 0.6 °C/sec (1 °F/sec) to over 56 °C/sec (100 °F/sec). In some cases the new and conventional methods differed by as much as 30 percent. Experimental and analytical results were compared to demonstrate the new technique. For heating conditions greater than 6 °C/sec (10 °F/sec), the indicated strain data corrected with the developed technique compared much better to analysis than the same data corrected with the conventional technique.

14. SUBJECT TERMS

Apparent strain, Measurement errors, Strain–gauge measurement, Structural testing, Thermal stress analysis

15. NUMBER OF PAGES

16

16. PRICE CODE

A02

17. SECURITY CLASSIFICATION OF REPORT	18. SECURITY CLASSIFICATION OF THIS PAGE	19. SECURITY CLASSIFICATION OF ABSTRACT	20. LIMITATION OF ABSTRACT
Unclassified	Unclassified	Unclassified	Unlimited